

Effect of moiré superlattice reconstruction in the electronic excitation spectrum of graphene-metal heterostructures

Antonio Politano^{1‡}, Guus J. Slotman^{2‡}, Rafael Roldán³,
Gennaro Chiarello¹, Davide Campi⁴, Mikhail I.
Katsnelson², Shengjun Yuan²

¹Department of Physics, Università della Calabria, I-87036 Rende, Italy

²Institute for Molecules and Materials, Radboud University, Heyendaalseweg
135, 6525AJ Nijmegen, The Netherlands

³Instituto de Ciencia de Materiales de Madrid, CSIC, Cantoblanco, E-28049
Madrid, Spain

⁴Department of Materials Science, University Milano-Bicocca, I-20125, Milano,
Italy

E-mail: antonio.politano@fis.unical.it, rroldan@icmm.csic.es,
s.yuan@science.ru.nl

Abstract. We have studied the electronic excitation spectrum in periodically rippled graphene on Ru(0001) and flat, commensurate graphene on Ni(111) by means of high-resolution electron energy loss spectroscopy and a combination of density functional theory and tight-binding approaches. We show that the periodic moiré superlattice originated by the lattice mismatch in graphene/Ru(0001) induces the emergence of an extra mode, which is not present in graphene/Ni(111). Contrary to the ordinary intra-band plasmon of doped graphene, the extra mode is robust in charge-neutral graphene/metal contacts, having its origin in electron-hole inter-band transitions between van Hove singularities that emerge in the reconstructed band structure, due to the moiré pattern superlattice.

Keywords graphene/metal interfaces, plasmons, moiré reconstruction, electron energy loss spectroscopy, tight-binding

Submitted to: *2D Mater.*

‡ Contributed equally to this work

Large-scale, highly crystalline graphene can be grown on metal substrates by chemical vapour deposition (CVD). [1] Depending on lattice mismatch between graphene (Gr) and the underlying substrate, graphene can grow as commensurate or incommensurate sheets. In the latter case, a moiré superlattice emerges [2]. The moiré-derived superperiodic potential leads to a reconstruction of the electronic band structure, with emergence of mini-bands and Dirac-cone replicas in the moiré superlattice Brillouin zone, leading to a wealth of intriguing phenomena [2, 3, 4, 5, 6]. The spatial modulation in periodically rippled graphene determines the existence of localized electronic states in the high and low areas of the moiré structure at energies close to the Fermi level [7]. The band structure reconstruction imposed by the periodic moiré potential implies a modification of screening properties and, thus, of the plasmonic excitations [8]. Inter-band transitions associated with the superlattice mini-bands contribute to the excitation spectrum of quasi-periodic Gr/hBN superlattices, as recently shown by infrared nano-imaging experiments [9]. Similar effects associated with the moiré pattern have been observed in the phonon spectra of Gr/Ru(0001) and Gr/Ni(111) [10, 11, 12]. Whereas optical experiments typically probe modes of small wave-vectors, of the order of the photon momentum, spectroscopies based on inelastic scattering of impinging electrons allow exploring the excitation spectrum along the whole Brillouin zone.

Herein, we take as model systems periodically rippled Gr/Ru(0001) and flat, commensurate graphene on Gr/Ni(111) to put in evidence the effects of the moiré reconstruction on plasmonic excitations in graphene. For this aim we combine high-resolution electron energy loss spectroscopy (HREELS) with theoretical *ab initio* density functional theory (DFT) and tight-binding propagation method (TBPM) calculations [13, 14]. Due to the lattice mismatch with the Ru lattice, graphene forms a moiré reconstruction on Ru(0001) [15, 16, 17], well approximated as a (12×12) . The geometric corrugation of graphene nanodomains on Ru(0001) has been imaged by scanning tunneling microscopy (STM) [16, 18]. Periodically inhomogeneous electronic properties in valleys and hills of the ripples have been inferred by means of scanning tunneling spectroscopy (STS) [19], which shows the occurrence of (i) localized states [7], (ii) splitting of image states [20] and (iii) local variations of the work function [21]. Peaks observed in STS near the Fermi level

arise from localized electronic states in the hills of the moiré pattern [7]. Conversely, the close lattice match between graphene and Ni allows the growth of a commensurate graphene overlayer on Ni(111) [22, 23, 24]. Despite the hybridization of Ni- $d_{3z^2-r^2}$ orbitals with π states of graphene [25], the adsorption energy still remains in the range of a typical physisorption (67 meV per carbon atom) [26]. We find that commensurate graphene on Ni(111) exhibits a single plasmon peak, associated to well known standard intra-band collective charge oscillation with dispersion $\hbar\omega_{pl} \propto \sqrt{q_{||}}$, in terms of the in-plane wave-vector $q_{||}$. On the other hand, Gr/Ru(0001) shows (besides the standard intra-band plasmon) an additional gapped and weakly dispersing mode in the spectrum. Our TBPM calculations, based on structures determined by atomistic simulations, suggest that the extra mode is associated to inter-band particle-hole excitations between van Hove singularities generated in the reconstructed band structure of the moiré superlattice.

HREELS experiments have been performed on graphene grown on single crystals of Ru(0001) and Ni(111), by dosing ethylene with the sample kept at 1050 and 790 K, respectively. For the case of moiré-reconstructed Gr/Ru(0001), periodic nanodomains have been imaged by STM, as we reported elsewhere [16]. HREELS experiments were carried out by using an electron energy loss spectrometer, whose energy resolution is 5 meV. The range of primary beam energies used for investigating the dispersion of low-energy plasmons, $E_p = 7 - 12$ eV, provided the best compromise among surface sensitivity, high cross-section for mode excitation and $q_{||}$ resolution. As given by $\hbar q_{||} = \hbar(k_i \sin \alpha_i - k_s \sin \alpha_s)$, the parallel momentum transfer $q_{||}$ depends on E_p , E_{loss} , α_i and α_s according to [27]:

$$q_{||} = \frac{\sqrt{2mE_p}}{\hbar} \left(\sin \alpha_i - \sqrt{1 - \frac{E_{\text{loss}}}{E_p}} \sin \alpha_s \right), \quad (1)$$

where E_{loss} is the energy loss, α_s is the electron scattering angle and k_i and k_s are the wave-vectors of impinging and of scattered electrons, respectively. All measurements were made at room temperature. Further experimental details are reported in the Supporting Information (SI).

Fig. 1a shows the HREELS spectra acquired for Gr/Ni(111) (blue curve) and Gr/Ru(0001) (green curve) for a primary electron beam energy $E_p = 7$ eV in an off-specular scattering geometry ($\alpha_i = 55^\circ$;

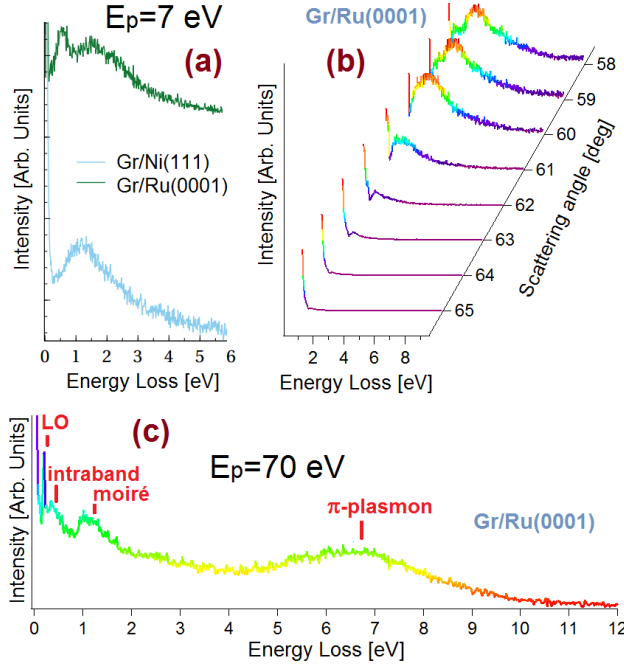


Figure 1. (a) HREELS spectra of graphene (Gr) on Ni(111) and on Ru(0001), acquired with an energy of the primary electron beam E_p of 7 eV; (b) Angle-resolved HREELS spectra for Gr/Ru(0001), acquired with $E_p = 7$ eV and for an incidence angle of 65° with respect to the sample normal; (c) Extended HREELS spectrum for Gr/Ru(0001), measured with $E_p = 70$ eV. The longitudinal optical (LO) phonon is also observed.

$\alpha_s = 49^\circ$). The loss spectrum of Gr/Ni(111) is characterized by a single peak [at an energy of 1.2 eV for $q_{||} = 0.12 \text{ \AA}^{-1}$, as obtained from Eq. (1)], assigned to the standard intra-band plasmon of doped graphene (for a review see e.g. [28, 29, 30]). Such a mode corresponds to the collective excitation of the charge density associated to graphene carriers screened by the Ni substrate [31]. The dispersion relation of this mode is that of plasmons in a two-dimensional electron gas (2DEG) [32] $\hbar\omega_{pl}(q_{||}) \approx \sqrt{\frac{2e^2\mu}{\epsilon_B}q_{||} + \frac{3}{4}v_F^2q_{||}^2}$, where μ is the chemical potential, $\epsilon_B = (1 + \epsilon_{\text{subs}})/2$, ϵ_{subs} being the dielectric constant of the substrate and v_F is the Fermi velocity of the carriers. In the long wavelength limit ($q \rightarrow 0$), the main difference is that the velocity of the plasmon mode in Gr/Ni(111), defined from the slope of the dispersion relation, is smaller as compared to isolated graphene, due to the screening effects of the Ni substrate. At large wave-vectors the dispersion of the mode is dominated by the linear term $\sim (3/4)^{1/2}v_Fq_{||}$.

Contrary to the excitation spectrum of graphene on Ni(111) that presents a single peak, our HREELS experiments for periodically rippled Gr/Ru(0001), as shown by the green line in Fig. 1a, show two loss features at 0.6 and 1.5 eV, corresponding to $q_{||} = 0.13$ and 0.21 \AA^{-1} in-plane wave-vectors, respectively. This

finding is an evident fingerprint of the deep difference in the electronic properties of the two epitaxial-graphene systems. By considering the values of the above-mentioned physical quantities for Gr/Ru(0001), we can assume that the peak at 0.6 eV corresponds to the standard intra-band plasmon of graphene, which is the counterpart in Gr/Ru(0001) of the mode discussed above for Gr/Ni(111). Here we are interested on elucidating the nature of the extra mode observed at ~ 1.5 eV, which will be the focus of our work. For this we have measured the dispersion relation of plasmonic excitations in Gr/Ru(0001), by collecting loss spectra as a function of the scattering angle at fixed incident angle ($\alpha_i = 65^\circ$) and with $E_p = 7$ eV. Fig. 1b shows that in nearly specular conditions ($\alpha_s = 65^\circ - 62^\circ$), i.e. for small momenta, the intraband plasmon is the unique peak which can be distinguished in the experimental loss spectrum. At $\alpha_s = 61^\circ$, the extra mode emerges ($q_{||} = 0.14 \text{ \AA}^{-1}$) and becomes the predominant peak of the HREELS spectrum for $\alpha_s = 60^\circ$.

We note that the so-called π -plasmon mode at 6 – 7 eV, originated from inter-band electron-hole transitions between the van Hove singularities of the graphene π -bands [33, 34, 35, 36], cannot be excited in the experimental conditions at which Fig. 1b has been obtained. However, by increasing the impinging energy E_p at 70 eV (Fig. 1c), the π -plasmon appears in the HREELS spectrum, while the cross-section for the excitation of low-energy plasmons is reduced at such a high value of the primary electron beam energy.

To establish whether the extra mode could be an effect of the moiré superlattice of Gr/Ru(0001), we have constructed a TB model of a deformed graphene layer, considering the positions of the carbon atoms in graphene nanodomains on Ru(0001), as obtained by DFT calculations (Fig. 2a) (see details in Sec. S3 of the SI). We then use this information to modulate the hopping parameters t_{ij} between sites i and j and on-site potentials v_i as function of interatomic distances of the different carbon atoms [37, 38]. The modulation of the on-site energy is shown in Fig. 2b, which follows the same periodicity as the modulation of the atomic coordinates in the moiré pattern. By repeating the unit cell shown in Fig. 2(a), we extended the superlattices to 6000×6000 carbon atoms, which is the typical size of our real space TB Hamiltonian matrix. After constructing the TB Hamiltonian for the Gr/Ru(0001), we calculate numerically the corresponding electronic density of states (DOS) by using the TBPM [13, 14]. Here the DOS is obtained by Fourier transform of the time-dependent correlation function $\langle \varphi | e^{-iHt} | \varphi \rangle$, where $|\varphi\rangle$ is a random initial wave function. The time-evolution in the correlation function is performed by using the Chebychev polynomial algorithm.

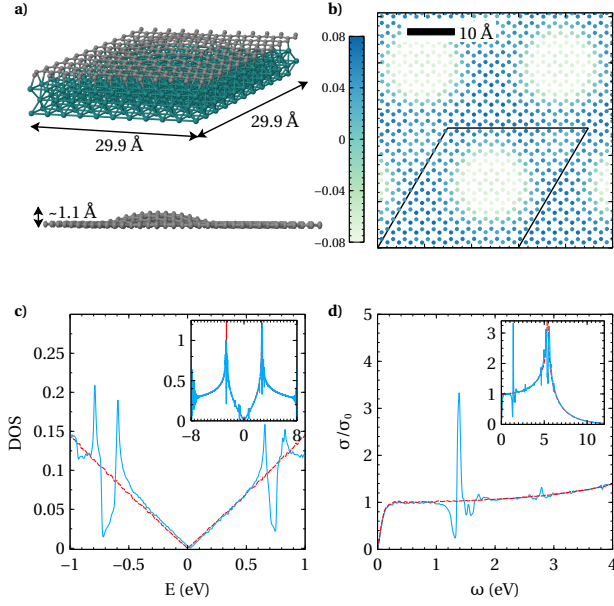


Figure 2. a) The structure of graphene on top of ruthenium as obtained by DFT calculations. A side view is given on the bottom to indicate the differences in height of the carbon atoms. b) The modified on-site potential in units of eV, with the DFT unit cell from a) highlighted. c) The density of states for Gr/Ru(0001) (blue), which present extra Van Hove singularities associated to the mini bands of the moiré superlattice. For comparison we show the corresponding DOS of a pristine graphene layer (red). The inset shows the DOS for a larger scale. d) The optical conductivity at $\mu = 0$ of Gr/Ru(0001) (blue) as compared to pristine graphene (red), in units of $\sigma_0 = \pi e^2/2h$. The inset shows the optical conductivity for larger scales.

The result for the DOS of Gr/Ru(0001) superlattices is shown in Fig. 2c, which clearly indicates the appearance of new singularities in the spectrum as compared to pristine graphene. One could identify some of them according to the super-periodicity of the moiré pattern. For example, the extra singularities around the energy $\approx \pm 0.675$ eV (see inset of Fig. 2c) follow the expression $E_D = \pm 2\pi\hbar v_F/(\sqrt{3}\lambda)$, where $\lambda \approx 20.8a$ is the length of the moiré's pattern in terms of the graphene interatomic distance $a = 1.42$ Å, and $v_F = 3at/2$ is the Fermi velocity in pristine graphene [39, 40]. The emergence of these extra singularities indicates the presence of flat bands in the band structure of the moiré superlattices, and may induce new strong optical excitations between the valence and conduction bands. This is indeed what we obtain in our numerical calculations for the optical conductivity shown in Fig. 2d, which have been obtained by using the Kubo's formula [41] in the framework of TBPM [13]. A very sharp optical excitation peak (absent in pristine graphene) appears at the energy $2|E_D| \approx 1.35$ eV. At the same time, the optical conductivity at an energy smaller than $2|E_D|$ rapidly drops from $3.3\sigma_0$ to $0.25\sigma_0$, where $\sigma_0 = \pi e^2/2h$ is the universal optical

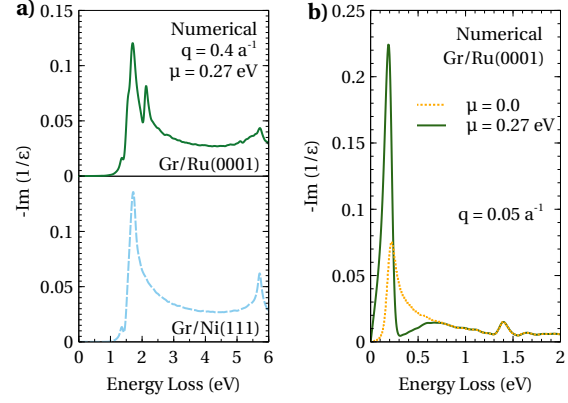


Figure 3. a) Numerical results of the energy loss function for Gr/Ru(0001) (above) as compared to Gr/Ni(111) (below). For Gr/Ru(0001) an extra peak in the loss function is observed. b) The loss function for Gr/Ru(0001) for two different charge doping, namely $\mu = 0$ (dashed yellow) and 0.27 eV (solid green). Notice that the extra peak is independent of μ .

conductivity of graphene. Such a phenomenon is qualitatively similar to that obtained in the infrared optical spectrum of Gr/h-BN heterostructures, due to the quasi-periodic moiré superlattice reconstruction, as it has been discussed theoretically [38] and observed experimentally [9]. Thus, periodically rippled graphene on Ru(0001) represents a suitable platform to modulate the optical properties of graphene.

In order to compare to the HREELS experiments of Fig. 1, we calculate the loss function $-\text{Im}(1/\epsilon)$, in terms of the dielectric function within the random phase approximation (RPA) $\epsilon(\mathbf{q}, \omega) = 1 - \frac{2\pi e^2}{q\epsilon_B} \Pi(\mathbf{q}, \omega)$, where $\Pi(\mathbf{q}, \omega)$ is the polarization function. Our theoretical results for Gr/Ni(111) and for Gr/Ru(0001) are shown in Fig. 3. The calculated loss function $-\text{Im}(1/\epsilon)$ of Gr/Ru(0001) (Fig. 3a) well reproduces the emerging extra mode of energy ~ 1.5 eV, which is instead absent in flat, commensurate Gr/Ni(111). This fact is in good agreement with our HREELS measurements, Fig. 1. This feature is due to a mode associated to transitions between electrons in the saddle points of the mini-bands generated by the moiré superlattice. When devising optoelectronic applications, the behavior of the modes with respect to modifications of the charge doping should be taken into account. We have further studied the effect of doping on the moiré mode. Fig. 3b shows that the extra inter-band mode is not affected by the carrier concentration, being present also in a charge-neutral moiré superlattice on Ru(0001). The robustness of the moiré mode toward changes in electron doping also implies that it would not be influenced by environmental doping, usually observed in air-exposed graphene field-effect transistors [43]. Experimentally,

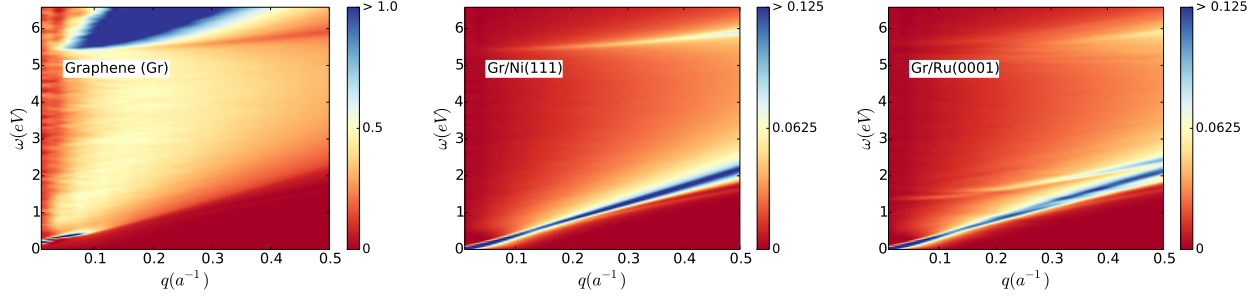


Figure 4. Loss function $-\Im(1/\epsilon(\mathbf{q}, \omega))$ calculated in steps of $0.01a^{-1}$ in q for angle $\theta = 0^\circ$. From left to right: Graphene, Gr/Ni(111), Gr/Ru(0001). For graphene and Gr/Ni(111) a flat, unrelaxed layer of graphene is used. For Gr/Ru(0001) the distortions caused by the substrate are also taken into account. Different dielectric screening constant are used, namely for graphene $\epsilon_B = 1$, and for Gr/Ni(111) and for Gr/Ru(0001), to mimic a metal substrate we have used $\epsilon_B = 80$. [42]

it is not possible to apply gate voltages in an HREELS apparatus and, thus, we are unable to probe plasmons in charge-neutral Gr/Ru(0001). However, HREELS studies on plasmonic modes in moiré-reconstructed, charge-neutral graphene on Pt₃Ni(111) reveal that only the moiré mode exists at this interface (Section S4, SI).

We notice that, strictly speaking, the moiré mode cannot be considered as *fully coherent plasmons*, as it is the case for the low-energy plasmon with dispersion law given by $\hbar\omega_{pl}(q_{\parallel}) \propto \sqrt{q_{\parallel}}$. For doped graphene (free-standing or deposited on any substrate), the intra-band $\sqrt{q_{\parallel}}$ plasmon is undamped above the threshold $\hbar\omega = v_F q$ until it enters the inter-band particle-hole continuum of the spectrum, and then it is damped by decaying into electron-hole pairs. However, the inter-band *moiré* mode that we have found in Gr/Ru(0001) is a mode which lies inside the continuum of particle-hole excitations: $-\text{Im}\Pi(q, \omega) > 0$ at the inter-band energy ω . Therefore, the mode is damped even in the limit $q \rightarrow 0$ (see also Sec. S7 of the SI). The phenomenology of this mode is similar to that of the so-called π -plasmon in graphene, that has been studied from both experimental [33, 34, 36] and theoretical [35] point of views, and it is observed also in our present experiments (Fig. 1c) and theoretical calculations (Fig. 4) at around 6 – 7 eV.

In Fig. 4 we compare the corresponding loss functions $-\Im(1/\epsilon(\mathbf{q}, \omega))$ in the $\omega - q$ plane, calculated with our model in the range of wave-vectors ($0.01a^{-1} \leq q \leq 0.5a^{-1}$) for momentum transfer \mathbf{q} along the Γ –K direction, corresponding to plasmon wavelengths in the range $\lambda_{pl} \sim 90 - 2$ nm. Plasmon dispersion in the Γ –M direction (reported in Figure S6 of the SI) is quite similar. Both, free-standing graphene and Gr/Ni(111) (Fig. 4a,b), are characterized by two modes: a low-energy intra-band plasmon (with dispersion relation given by $\hbar\omega_{pl}(q_{\parallel}) \approx \sqrt{\frac{2e^2\mu}{\epsilon_B} q_{\parallel} + \frac{3}{4}v_F^2 q_{\parallel}^2}$), and a high-energy inter-band π -plasmon [33, 34, 35]. As seen in Fig. 4, the dispersion

of the standard low-energy 2D plasmon for all the cases is dominated, at large wave-vectors, by the linear term $\sim \sqrt{3/4}v_F q_{\parallel}$, which is independent of the dielectric constant of the embedding medium. Periodically rippled Gr/Ru(0001) (Fig. 4c) exhibits, besides the above-mentioned modes, an extra mode dispersing from 1.7 eV at $q = 0$ to 2.3 eV at high momenta. As we have discussed above, we associate this mode to the HREELS peak in the loss function at this energy (Fig. 1). It is interesting to notice that a careful inspection of Fig. 4c also indicates the occurrence of moiré-derived splitting of the high-energy inter-band π -plasmon. The HREELS spectrum shown in the SI, Fig. S8, indicates that also such a theoretical prediction well reproduces the experimental findings.

In conclusion, we have studied the influence of moiré superlattice on the excitation spectrum of Gr/metal contacts. Whereas Gr/Ni(111) shows commensurate lattices with no relevant effect on the band structure, Gr/Ru(0001) leads to a moiré superlattice with a reconstruction of the energy band spectrum of graphene. In particular, new flat mini-bands are created, which produce the appearance of van Hove singularities in the electronic DOS. Our HREELS experiments reveal extra peaks in the loss spectrum of Gr/Ru(0001), which are well explained by our theoretical model based on TBPM. We associate the extra modes to inter-band excitations between the newly generated van Hove singularities. Our results demonstrate the importance of the band reconstruction in the excitation spectrum of graphene on specific substrates, associated to the moiré-derived superperiodic potential. The evidence of extra modes in graphene quantum dots paves the way toward the control of graphene plasmonic properties through appropriately engineered periodic surface patterns. Moreover, the occurrence of an extra mode in the visible range of the spectrum, robust against environmental doping, opens novel perspectives for graphene optoelectronics.

Acknowledgments

A.P. and G.J.S. contributed equally to this work. AP and GC thank Fabio Vito for technical support in HREELS experiments. The support by the Netherlands National Computing Facilities foundation (NCF) are acknowledged. S.Y. and M.I.K. thank financial support from the European Research Council Advanced Grant program (contract 338957). The research has also received funding from the European Union Seventh Framework Programme under Grant Agreement No. 604391 Graphene Flagship. R.R. acknowledges financial support from MINECO (Spain) through grant FIS2014-58445-JIN.

The Supporting Information is available free of charge on the IOP Publishing website at DOI:(to be filled) The SI reports additional information on the TB model; additional experimental details; the coordinates of the graphene nanodomains on Ru(0001); Gr/Pt₃Ni(111); dynamical polarization function and dispersion relation in the other symmetry directions; splitting in the π -plasmon; estimate of the damping of the moiré plasmon mode; loss spectra of clean Ru(0001); and STM visualization of periodically rippled Gr/Ru(0001). (PDF)

References

- [1] Batzill M 2012 *Surf. Sci. Rep.* **67** 83 – 115
- [2] Pletikosić I, Kralj M, Pervan P, Brako R, Coraux J, N'Diaye A T, Busse C and Michely T 2009 *Phys. Rev. Lett.* **102**(5) 056808
- [3] Xu Y, Semidey-Flecha L, Liu L, Zhou Z and Goodman D W 2011 *Farad. Discuss.* **152** 267–276
- [4] Voloshina E N, Fertitta E, Garhofer A, Mittendorfer F, Fonin M, Thissen A and Dedkov Y S 2013 *Sci. Rep.* **3** 1072
- [5] Wallbank J R, Patel A A, Mucha-Kruczyński M, Geim A K and Fal'ko V I 2013 *Phys. Rev. B* **87**(24) 245408
- [6] San-Jose P, Gutiérrez-Rubio A, Surla M and Guinea F 2014 *Phys. Rev. B* **90**(7) 075428
- [7] Stradi D, Barja S, Díaz C, Garnica M, Borca B, Hinarejos J J, Sánchez-Portal D, Alcamí M, Arnau A, Vázquez de Parga A L, Miranda R and Martín F 2012 *Phys. Rev. B* **85**(12) 121404
- [8] Tomadin A, Guinea F and Polini M 2014 *Phys. Rev. B* **90**(16) 161406
- [9] Ni G X, Wang H, Wu J S, Fei Z, Goldflam M D, Keilmann F, Özyilmaz B, Castro Neto A H, Xie X M, Fogler M M and Basov D N 2015 *Nat. Mater.* **14** 1217
- [10] Maccariello D, Campi D, Al Taleb A, Benedek G, Fariás D, Bernasconi M and Miranda R 2015 *Carbon* **93** 1–10
- [11] Maccariello D, Al Taleb A, Calleja F, Vázquez de Parga A, Perna P, Camarero J, Gneco E, Farias D and Miranda R 2015 *Nano letters* **16** 2–7
- [12] al Taleb A, Anemone G, Fariás D and Miranda R 2016 *Carbon* **99** 416–422
- [13] Yuan S, De Raedt H and Katsnelson M I 2010 *Phys. Rev. B* **82** 115448
- [14] Hams A and De Raedt H 2000 *Phys. Rev. E* **62** 4365
- [15] Wang B, Bocquet M L, Marchini S, Günther S and Wintterlin J 2008 *Phys. Chem. Chem. Phys.* **10** 3530–3534
- [16] Borca B, Barja S, Garnica M, Minniti M, Politano A, Rodríguez-García J M, Hinarejos J J, Fariás D, Vázquez de Parga A L and Miranda R 2010 *New J. Phys.* **12** 093018
- [17] Iannuzzi M, Kalichava I, Ma H, Leake S J, Zhou H, Li G, Zhang Y, Bunk O, Gao H, Hutter J, Willmott P R and Greber T 2013 *Phys. Rev. B* **88**(12) 125433
- [18] Marchini S, Günther S and Wintterlin J 2007 *Phys. Rev. B* **76** 075429
- [19] Gyamfi M, Eelbo T, Waśniowska M and Wiesendanger R 2011 *Phys. Rev. B* **83** 153418
- [20] Borca B, Barja S, Garnica M, Sánchez-Portal D, Silkin V M, Chulkov E V, Hermanns C F, Hinarejos J J, Vázquez de Parga A L, Arnau A, Echenique P M and Miranda R 2010 *Phys. Rev. Lett.* **105**(3) 036804
- [21] Feng W, Lei S, Li Q and Zhao A 2011 *J. Phys. Chem. C* **115** 24858–24864
- [22] Shikin A, Farias D, Adamchuk V and Rieder K H 1999 *Surf. Sci.* **424** 155–167
- [23] Gamo Y, Nagashima A, Wakabayashi M, Terai M and Oshima C 1997 *Surf. Sci.* **374** 61–64
- [24] Dahal A and Batzill M 2014 *Nanoscale* **6** 2548–2562
- [25] Andersen M, Hornekær L and Hammer B 2012 *Phys. Rev. B* **86**(8) 085405
- [26] Mittendorfer F, Garhofer A, Redinger J, Klimeš J, Harl J and Kresse G 2011 *Phys. Rev. B* **84**(20) 201401
- [27] Rocca M 1995 *Surf. Sci. Rep.* **22** 1 – 71
- [28] Grigorenko A N, Polini M and Novoselov K S 2012 *Nature Photon.* **6** 749–758
- [29] Stauber T 2014 *J. Phys.: Condens. Matter* **26** 123201
- [30] Politano A and Chiarello G 2014 *Nanoscale* **6** 10927–10940
- [31] Cupolillo A, Ligato N and Caputi L 2013 *Surf. Sci.* **608** 88 – 91
- [32] Stern F 1967 *Phys. Rev. Lett.* **18**(14) 546–548
- [33] Eberlein T, Bangert U, Nair R R, Jones R, Gass M, Bleloch A L, Novoselov K S, Geim A and Briddon P R 2008 *Phys. Rev. B* **77**(23) 233406
- [34] Politano A, Radović I, Borca D, Mišković Z and Chiarello G 2016 *Carbon* **96** 91 – 97
- [35] Yuan S, Roldán R and Katsnelson M I 2011 *Phys. Rev. B* **84** 035439
- [36] Nelson F J, Idrobo J C, Fite J D, Miskovic Z L, Pennycook S J, Pantelides S T, Lee J U and Diebold A C 2014 *Nano Letters* **14** 3827–3831
- [37] Pereira V M, Castro Neto A H and Peres N M R 2009 *Phys. Rev. B* **80** 045401
- [38] Slotman G J, van Wijk M M, Zhao P L, Fasolino A, Katsnelson M I and Yuan S 2015 *Phys. Rev. Lett.* **115**(18) 186801
- [39] Park C H, Yang L, Son Y W, Cohen M L and Louie S G 2008 *Phys. Rev. Lett.* **101**(12) 126804
- [40] Park C H, Yang L, Son Y W, Cohen M L and Louie S G 2008 *Nat. Phys.* **4** 213–217
- [41] Kubo R 1957 *J. Phys. Soc. Jpn.* **12** 570–586
- [42] Choi W S, Seo S S A, Kim K W, Noh T W, Kim M Y and Shin S 2006 *Phys. Rev. B* **74** 205117
- [43] Yang Y, Brenner K and Murali R 2012 *Carbon* **50** 1727